

Proton Beam Nano-Machining: End Station Design and Testing

J.A. van Kan¹, A.A. Bettiol and F. Watt
Centre for Ion Beam Applications, Physics Department,
National University of Singapore, Singapore 117542
¹Contact: phyjavk@nus.edu.sg

ABSTRACT

A new nuclear nanoprobe facility has been developed at the Centre for Ion Beam Applications (CIBA) in the Physics Department of the National University of Singapore. This facility is the first of its type dedicated to proton beam micromachining on a micron as well as a nano scale. The design and performance of the facility, which is optimized for 3D lithography with MeV protons, is discussed here. The system has been designed to be compatible with Si wafers up to 6".

The production of good quality high aspect ratio microstructures requires a lithographic technique capable of producing microstructures with smooth vertical sidewalls. In proton beam micromachining, a high energy (e.g. 2 MeV) proton beam is focused to a sub-100 nm spot size and scanned over a resist material (e.g. SU-8 and polymethylmethacrylate (PMMA)). When a proton beam interacts with matter it follows an almost straight path, the depth of which is dependent on the proton beam energy. These features enable the production of nanometer sized polymer structures. Experiments have shown that post-bake and curing steps are not required in this SU-8 process, reducing the effects of cracking and internal stress in the resist. Since proton beam micromachining is a fast direct write lithographic technique it has high potential for the production of high-aspect-ratio nano-structures.

INTRODUCTION

Current microelectronics production technologies are essentially two-dimensional (2D), well suited for the 2D topologies prevalent in microelectronics. As semiconductor devices are scaled down in size, coupled with the integration of moving parts on a chip, there will be an increasing demand for smaller Micro Electro Mechanical System (MEMS) devices. High aspect ratio three-dimensional (3D) microstructures with sub-micron details are also of growing interest for optoelectronic devices. Therefore it is essential to develop new lithographic techniques suitable for the production of high aspect ratio 3D micro- and nano-components. One of the more established techniques for 3D micromachining is X-ray lithography with electroforming and micromoulding (LIGA) [1] although one drawback for this process is the relative high production cost involved coupled with the scarcity of facilities. There are a few emerging new lithographies (e.g. Proton Beam writing (p-beam writing), deep ultra violet (DUV) lithography and stereo microlithography). P-beam writing is being developed at the CIBA and has the potential to be a promising new 3D lithographic technique [2-4]. In p-beam writing, a high energy (e.g. 2 MeV) proton beam is focused to a sub-micron spot size and scanned over a suitable resist material (e.g. SU-8 and PMMA), to produce a 3D latent image in a resist material. Of these new techniques p-beam writing is the only technique that offers the capability of direct write high aspect ratio nano- and microstructures. P-beam writing is a fast direct write lithographic technique; in a few seconds a complicated pattern in an area of 400 x 400 μm^2 can

be exposed down to a depth of, for example, 150 μm . These features make p-beam writing a direct write technique of high potential for the production of high-aspect-ratio structures with sub-100 nm detail in lateral directions at a much lower total cost than the LIGA process, which requires a synchrotron radiation source and precision masks. Recently in the CIBA, a new dedicated system which is optimized for lithography with MeV protons has been designed and tested. This system is the first of its kind in the world. The focus of this paper will be mainly on the design of the hardware and the first exposures performed with this new system. The first tests show it is possible to use focused MeV proton beams to direct write 3D nano structures (e.g. sub-100 nm).

HARDWARE DESIGN

A schematic overview of the proton beam micromachining facility used is shown in figure 1. Protons from a nuclear accelerator are focused down to sub-100 nm spot sizes and are used to

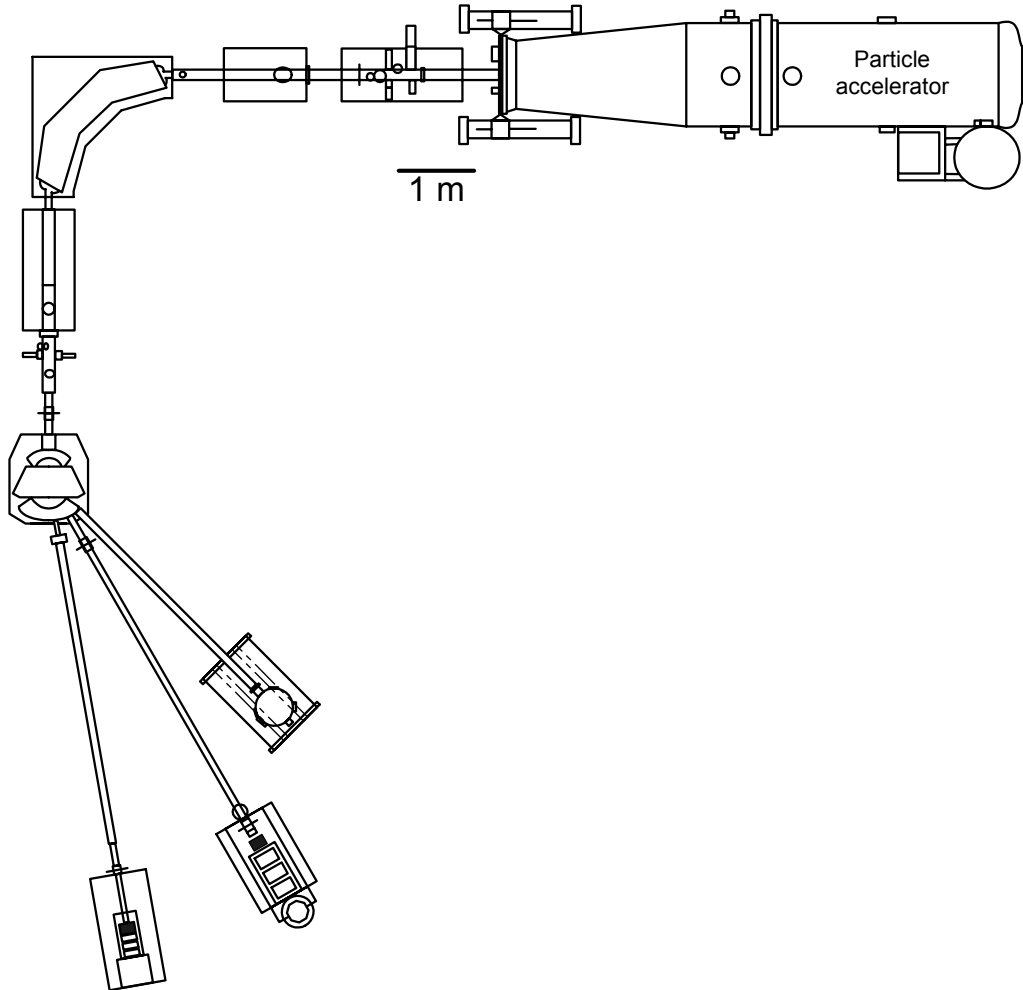


Figure 1. Schematic diagram of the accelerator facility at the CIBA. The p-beam writing beam line is at 10° with respect to the switcher magnet.

direct write patterns in resist materials. Recently the p-beam writing has been improved substantially with the introduction of a state of the art, high brightness, 3.5 MV single-ended accelerator (HVEE Singletron). This new machine produces proton beams of much higher stability and brightness than the belt driven Van de Graaff accelerator previously used for micromachining purposes.

The protons from the accelerator are energy analyzed using the 90° magnet. Beam defining object slits are positioned one meter in front of the switcher magnet. Here we can set a rectangular object aperture, such that the transmitted beam through the aperture is de-magnified with a set of magnetic quadrupole lenses located directly in front of the target chamber and the demagnified image transmitted into the target chamber. An electro static beam deflection system is installed after the object slits which serves as a shutter. Using the switcher magnet the protons can be steered into the 30° nuclear microscope beam line, which is designed for microscopy purposes and has been used over the last few years for the development of proton beam micromachining. At 45° with respect to the switcher magnet we have also recently installed a materials characterization system which utilizes non-focused ion beams for Rutherford Backscattering studies. The protons can also be steered into the 10° beam line, the new P-beam writing facility dedicated to micro- and nano-machining. The P-beam writer utilizes the Oxford Microbeams high demagnification lenses (OM52) in a high excitation triplet configuration. This lens system operates at an object distance of 7 m and a reduced image distance of 70 mm resulting in enhanced system demagnifications (228x60 in the X and Y directions respectively). Because of the short working distance between the lens and the target, the optical microscope installed to check the position of the target has a limited magnification due to adverse geometrical considerations. The target chamber and focusing lens system is installed on an optical table to reduce vibrations. The sample is mounted on a computer controlled Burleigh Inchworm XYZ stage which has a travel of 25 mm for all axes with a 20 nm closed loop resolution. The system has been designed to be compatible with Si wafers up to 6". This new focusing system is able to produce proton beams down to a sub-100 nm spot size, which can be used for maskless direct write lithography.

During exposures the beam is scanned over the resist using a set of electromagnetic scan coils, located directly in front of the quadrupole lens system. In this way scan fields up to 1 x 1 mm² can be achieved. The first tests with the new system utilized only magnetic scanning. Since magnetic scanning systems have a relatively long settling time due to the magnetic scan coils resulting in a relative slow writing speed, we are currently installing a faster electrostatic scanning system to allow us to reduce exposure times. In addition, we have also been utilizing stage scanning which allows us to scan the beam over the full 25 x 25 mm² range of the XYZ stage. A typical exposure rate for SU-8 in the current system is about 1500 s/mm². In the optimized set-up, at state-of-the-art proton current densities of 1 nA/μm² exposure rates controlled via electrostatic scanning are expected to be as fast as 20 s/mm², while still maintaining micron resolution in the lateral direction.

The scan system utilizes a newly installed National Instruments NI 6731 Multi i/o card which has four 16 bit digital to analog converters (DACs) and has a minimum update time of 1.0 μs. The old card had 12 bit DACs. Two channels control the scan coils and a third DAC controls the beam deflection. This improved resolution is necessary to cope with the reduced beam spot size available in the new dedicated proton beam micromachining beam line. The scan software supports AUTOCAD and Bitmap file format; more details about the scanning system can be found elsewhere [5].

To guarantee a constant proton dose per pixel as the beam is digitally scanned across the resist, we have developed two main methods for dose normalization. Both methods rely on the detection of Rutherford Backscattering (RBS) signals. In the first method the beam is moved to a new position in a scan after a fixed number of backscattered protons has been detected (pixel normalization). In the second method the beam is scanned rapidly over a figure for many times until a sufficient dose has been reached (figure scanning). In both cases the average dose per area can be chosen in the scanning program. To facilitate the production of nano structures with smooth sidewalls, it is advantageous to use more sensitive feedback for normalization purposes. In the new system, provision is made to use signals such as secondary electron emission and ion induced photon emission which typically have a much higher yield per proton compared to the number of nuclear backscattered events per proton.

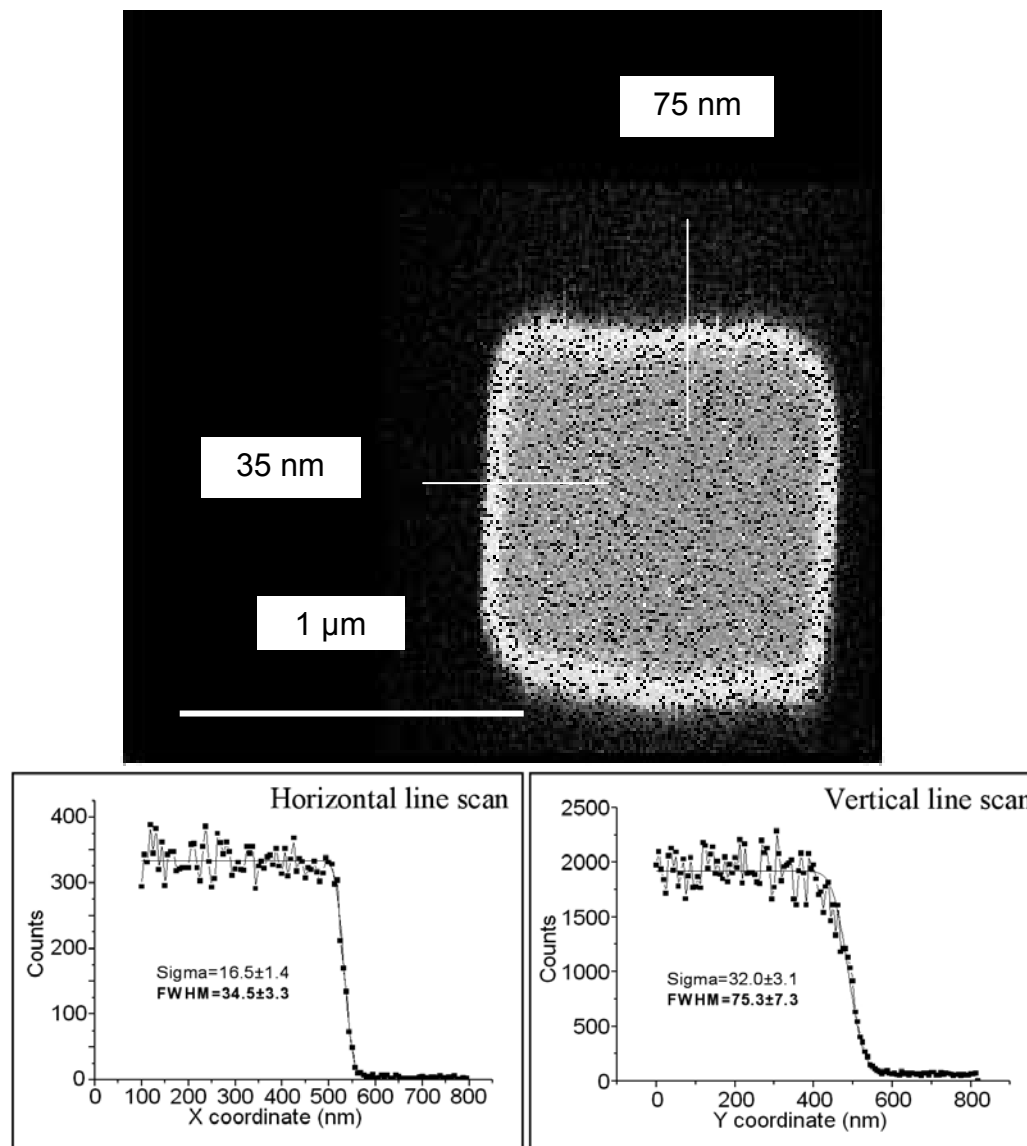


Figure 2. 2D map of forward scattered protons from a 1 μm hole etched into Si. The bottom part shows line scans indicating a beam spot size of 35 x 75 nm².

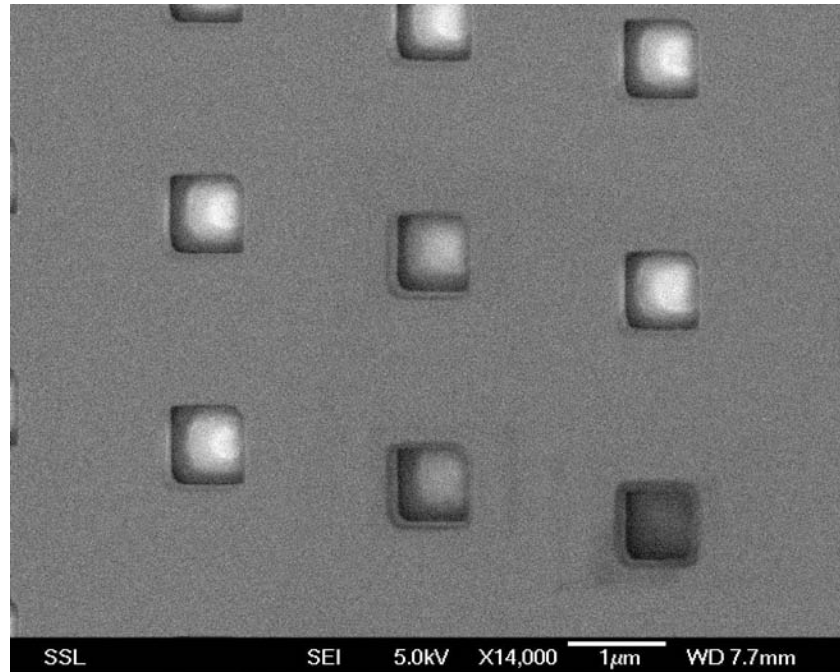


Figure 3. SEM image of the 1 μm holes in Si used to determine the beam spot size of the proton beam.

In the first tests with this system the focusing power of the new lenses was tested, see figure 2. A beam of 1 MeV protons was scanned over a 2 μm thick free standing X-ray mask which contains 1 x 1 μm^2 holes. Protons which passed through the holes in the mask were detected using a silicon surface barrier detector. De-convolution of line scans perpendicular to the edge of a 1 μm hole, which are assumed to be sharp and vertical, indicate a beam spot size of 35 x 75 nm^2 . In figure 3 we see a scanning electron micrograph (SEM) image of the X-ray mask used to de-convolute the beam spot size. The SEM micrographs indicate that the side walls of the holes are not perfect, but have a natural width profile of about 30 nm. This represents a limiting factor in the determination of the beam spot size.

The focused proton beam has a specific angular divergence which is dependent on beam optical parameters and the beam current density. In the horizontal plane (the high demagnification direction) a typical beam divergence on target is 1.5 mrad. According to earlier calculations [6] the beam has a spread in the resist material of less than 6 mrad in the first 5 μm , which enables p-beam writing to make structures with a side wall of better than 89.6° . Nanomachining at high accuracy requires the development of a focusing protocol, which ideally should include computer software for beam spot optimization, and high quality resolution standards. Both of these are currently being developed at CIBA.

RESIST EXPOSURE

In p-beam writing the path of a high energy (MeV) proton in material is dependent on the interaction with the electrons and nuclei in the material. The probability that a proton interacts with an electron is a few orders of magnitude higher than for nuclear scattering in the first 50% of its trajectory. Therefore only proton-electron interactions need to be considered in the first part of the proton trajectory. Proton-electron interactions hardly change the trajectory of a proton

because of the mass ratio ($m_p/m_e \sim 1800$), which implies that the path of a proton hardly deviates from a straight line. Since the energy transfer in these collisions is rather small, peaked at around 100 eV, many collisions will occur before a proton comes to rest. Proton trajectories can therefore be accurately simulated by means of Monte Carlo calculations, for example using the computer code TRIM [7]. The physical characteristics of ion/electron interactions make p-beam writing a predictable and an extremely powerful lithographic technique with the following key features:

Protons have a relatively large and well defined range in resist materials. For example by choosing a proton energy of 1.0 MeV or 3.5 MeV, structures with a height of 20 μm and 160 μm respectively can be produced, allowing the production of slots, holes and buried microchannels. Tilting the sample allows the production of non parallel microstructures. The virtual absence of small angle scattering in the initial path of the proton beam allows the production of high aspect ratio structures. Calculations [6] have shown that a 3.5 MeV proton beam will spread less than 100 nm in a 10 μm thick layer of resist. Finally there is a relatively constant energy deposition along the proton track which ensures uniform exposure rates along the initial path of the proton beam, again a requirement for the production of high quality nano- and micro-structures with high aspect ratio.

In p-beam writing experiments, we have used SU-8 and PMMA resist. SU-8 obtained from MicroChem Corp. (MCC) is spincoated on Si wafers. In order to make 200 nm layers of SU-8 the SU-8 5 was diluted in two parts per volume of Gamma Butyrolactone and spincoated for 2 minutes at 3000 rpm [8].

During irradiation the proton induced electrons will cross link the SU-8 resist or chain scission the molecular chains in PMMA resist. After the irradiation the resist will be developed; for PMMA samples the procedure given in [9] was followed and for the SU-8 samples the

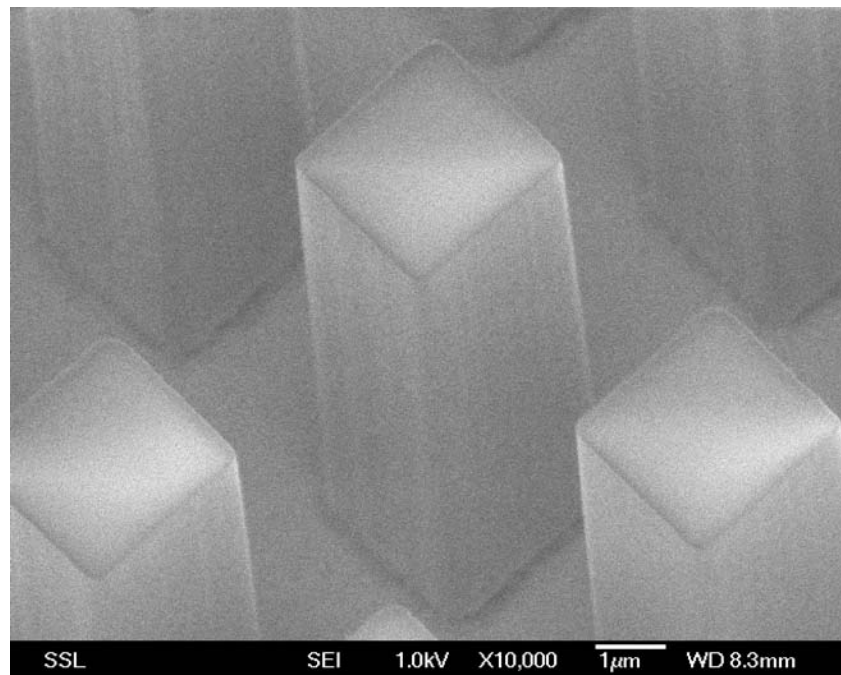


Figure 4. SEM image of $2.5 \times 2.5 \mu\text{m}^2$ squares in 10 μm thick SU-8, written with a focused 2 MeV proton beam.

standard developer from MCC was used at room temperature. Note that in the case of SU-8 no post exposure bake was used. Tests with post exposure bake have shown that structures with fine details (< 500 nm) are destroyed during post exposure bake.

DESIGN OF A NEW RESOLUTION STANDARD

Early resolution standards produced using p-beam writing [10] were p-beam machined from $15 \times 15 \mu\text{m}^2$ squares, and Ni plated to form a $15 \mu\text{m}$ thick Ni grid of high aspect ratio. These resolution standards proved too coarse for the improved performance of the new p-beam writing facility. These standards had a side wall angle of 89.5° corresponding to a projected side wall width of 130 nm. In a subsequent attempt at producing better resolution standards, we designed $2.5 \times 2.5 \mu\text{m}^2$ squares which were written in a $10 \mu\text{m}$ thick SU-8 layer applied on a conductive substrate. Figure 4 is a high magnification SEM photograph of a section of a matrix of 7 by 7 of these squares. They were produced with a 2 MeV proton beam which was focused down to a spot size of $200 \times 200 \text{ nm}^2$. The squares were written in an area of $50 \times 50 \mu\text{m}^2$ utilizing a $25 \times 25 \text{ nm}^2$ pixel size, the number of protons used for the exposure was 60 nC/mm^2 . Since we use a much smaller pixel size compared to the beam size, the deposited energy along the edge of the squares is less compared to the centre part, and so to ensure enough crosslinking along the edges a double dose compared to the normal dose was used. In future experiments a more elaborated study will be performed to establish the effect of an increased edge irradiation on the smoothness of the structures. As can be seen, the squares have a very high degree of smoothness, with sharp corners and near 90° side walls. As a next step, we will plate Ni around these squares at heights

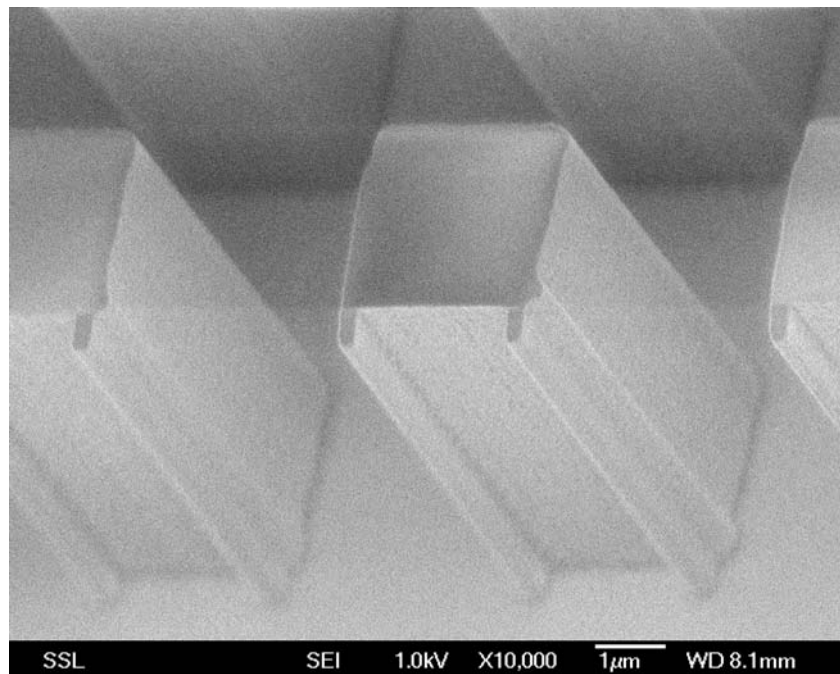


Figure 5. SEM image of $2.5 \times 2.5 \mu\text{m}^2$ squares in $10 \mu\text{m}$ thick SU-8 written with a focused 2 MeV proton beam. Perpendicular to these squares 200 nm wide walls were written along the edge of the squares.

of 200 nm – 1 micron. This will limit the slope in the side walls of the Ni structures to less than 10 nm, and will give us a more defined and sharper edge definition than previously realized.

HIGH ASPECT RATIO NANO STRUCTURES

In the next experiment $2.5 \times 2.5 \mu\text{m}^2$ squares were written in a $10 \mu\text{m}$ thick layer of SU-8, under similar conditions as the squares shown in figure 4. After writing the squares an extra line was written along the edges of the squares with a beam of $200 \times 200 \text{ nm}^2$. As can be seen in figure 5 the single line gives rise to a narrow wall of 200 nm width. This corresponds to an extremely high aspect ratio in SU-8 of 50. We believe this to be state-of-the-art performances in SU-8; only Bogdanov and Peredkov [8] have reported similar aspect ratios for SU-8 structures with a width of $4 \mu\text{m}$ or more.

As a first test to determine the lithographic capability of our new p-beam writing system, nano structures were written in a 200 nm thick layer of SU-8 spincoated on a Si wafer. In this layer a set of parallel lines were written with a beam of $120 \times 250 \text{ nm}^2$. The test structure was written with a 2 MeV proton beam in an area of $40 \times 40 \mu\text{m}^2$, the figure was digitized in a grid of 2048×2048 pixels of $20 \times 20 \text{ nm}^2$ each. The lines are 170 nm wide and 3000 nm long. The distance between the lines was varied to test the minimum gap size. Next to the parallel lines a set of orthogonal lines was also written. As can be seen in figure 6, all the structures appear relatively smooth and well defined. These structures were written with a 2 MeV proton beam using 30 nC/mm^2 .

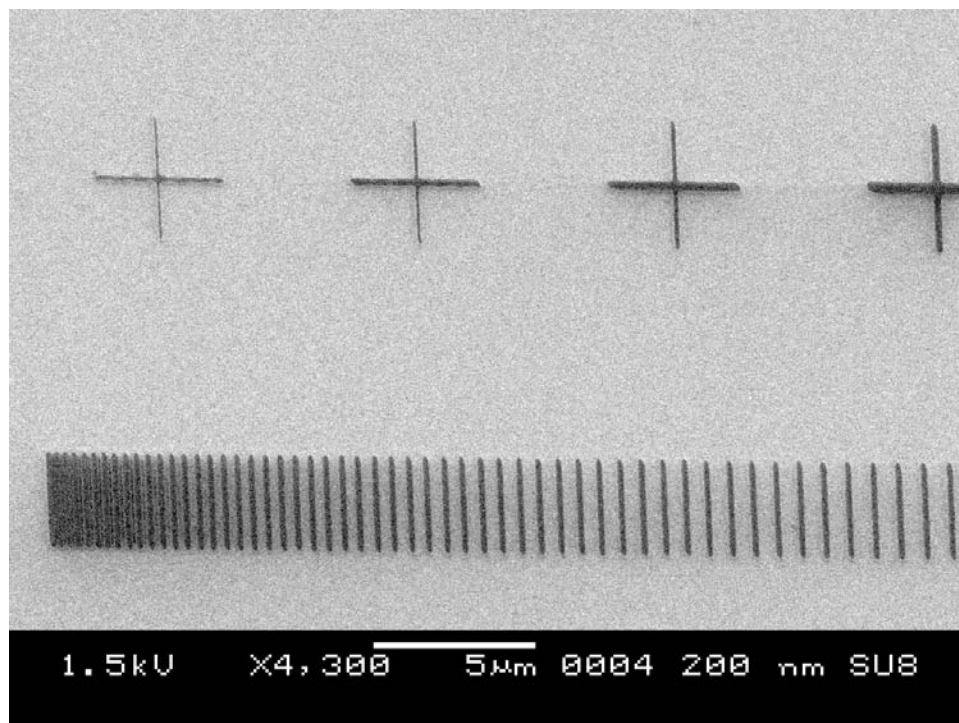


Figure 6. SEM image of a test pattern written in 200 nm thick SU-8 with a focused 2 MeV proton beam.

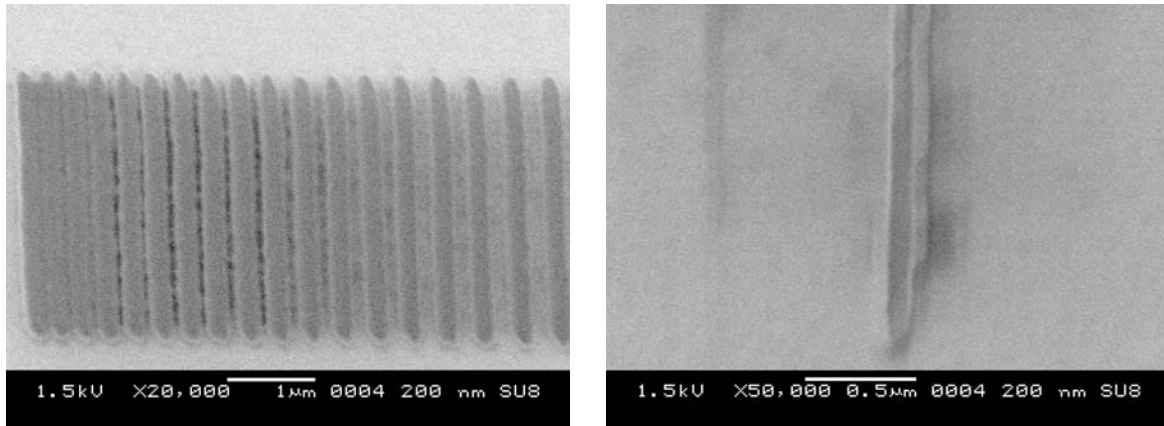


Figure 7. (Left) High magnification of the parallel lines in figure 6. (Right) High magnification of the narrowest cross, showing a width of 90 nm.

Figure 7 shows two high magnification SEM photographs of small details in the test structure. In figure 7 (left) it is clear that the lines get closer together till they are merged completely at the left side of the figure. The smallest gap is about 50 nm to 80 nm but the exact spacing is very difficult to ascertain. The problem in obtaining reliable sizes is the fact that SU-8 tends to evaporate during conventional SEM imaging. Atomic Force Microscopy (AFM) is not a very good alternative since the high aspect ratio of the SU-8 structures limits the imaging performance. To overcome these limitations, we intend to plate the spaces between the SU-8 with Ni, after which the SU-8 will be removed. Imaging of this type of metal structure will be easier using a SEM. A high magnification SEM photo of the vertical bar of the smallest cross in figure 6 is shown in figure 7 on the right. The width of the bar is 90 nm which we believe to be the smallest ever written single line in SU-8 [8,11].

Interestingly, during these experiments the de-convoluted beam spot size was measured to be $120 \times 250 \text{ nm}^2$ using the X-ray mask standard. Since the written line was observed to be 90 nm using SEM measurements, the measured beam spot size was therefore overestimated, indicating that the edge definition of the X-ray mask used as a resolution standard was around 30 nm, in keeping with the observations above. These findings suggest that our best results obtained in focusing a proton beam down to $35 \times 75 \text{ nm}^2$ is very conservative since we used the X-ray mask standard without correction for the edge width. It is therefore expected that an improved resolution standard will allow us to both measure and achieve a smaller beam focus and subsequently write even smaller nano sized structures.

CONCLUSIONS

Here we discussed the successful introduction of the world's first proton beam micromachining (p-beam writing) facility. In this system the proton beam can be focused down to $35 \times 75 \text{ nm}^2$ and directly scanned across a resist, thereby eliminating the need for a mask. This resolution is currently the best performance in the world for MeV protons [12]. Arbitrary shapes can be fabricated, high-aspect-ratios (more than 100) can be achieved in PMMA and SU-8 resist, and the smallest single line achieved so far in a 200 nm thick SU-8 layer is 90 nm.

Tests were performed which show that p-beam writing can potentially produce new resolution standards which will then improve the reproducibility of p-beam writing. These resolution standards will give a better estimate of the beam size.

The scanning speed in the new p-beam writing facility is expected to increase by a few orders of magnitude with the introduction of an electrostatic scanning system, avoiding the long settling times needed in the current magnetic scanning system. Although p-beam writing is in general slower than masked processes for bulk production, it is very suitable for rapid prototyping and in particular the manufacture of molds and stamps that can be used for batch and high-volume production.

With the new HVEE 3.5 MV accelerator, deep structures up to 160 μm can be produced with 3.5 MeV protons. The new machine, because of its increased beam brightness and high energy stability, has opened the way to even more precise micro- and nano-structures. The proton beam has a well defined range in resist (unlike x-rays), and therefore the depth of structures can be easily controlled by using different proton energies enabling the construction of slots, channels, holes etc. with a well defined depth. The depth can be different for slots, channels or holes in one single resist layer. In addition, by changing the angle of the resist with respect to the beam, complex shapes can be machined with very well defined sharp edges.

REFERENCES

- [1] F. Cerrina, in: P. Rai Choudury (Ed.), *Handbook of Microlithography, Micromachining and Microfabrication*, vol. 1, Ch.3, SPIE Press Monograph PM39, pp. 251-319, 1997.
- [2] F. Watt, J.A. van Kan, T. Osipowicz, *MRS Bulletin* February, 33 (2000).
- [3] J.A. van Kan, J.L. Sanchez, T. Osipowicz and F. Watt, *Microsystem Technologies*, **6**, 82 (2000).
- [4] J.A. van Kan, A.A. Bettiol and F Watt, submitted to APL.
- [5] A.A. Bettiol, J.A. van Kan, T.C. Sum and F. Watt, *Nucl. Instr. and Meth. B*, **B181**, 49 (2001).
- [6] J.A. van Kan, T.C. Sum, T. Osipowicz and F. watt, *Nucl. Instr. and Meth.* **B161-163**, 366 (2000).
- [7] J. Biersack and L.G. Haggmark, *Nucl. Instr. and Meth.* **174**, 257 (1980).
- [8] A.L. Bogdanov & S.S. Peredkov, <http://www.maxlab.lu.se/beamlines/bld811>.
- [9] S.V. Springham, T. Osipowicz, J.L. Sanchez, L.H. Gan and F. Watt, *Nucl. Instr. and Meth.* **B130**, 155 (1997).
- [10] F. Watt, I. Rajta, JA van Kan, AA Bettiol, T. Osipowicz, *Nucl. Instr. and Meth.* **B190**, 306 (2002).
- [11] T.W. Odom, V.R. Thalladi, J. Christover Love & G.M. Whitesides, *J AM Chem Soc* **124**, No 41, 12112 (2002).
- [12] F. Watt, J.A. van Kan, I. Rajta, A.A. Bettiol, T.F. Choo, M.B.H. Breese and T. Osipowicz, In press *Nucl. Instr. and Meth.*